Population pharmacokinetics of high-dose methotrexate using deep learning analysis of CT scan radiomics and biometric and laboratory data: the PREDICT-MTX study

PERIOD OF INTERNSHIP
April 10th, 2023 -June 30th, 2023

NAME STUDENT
Solaiman Ezzafzafi

STUDENTNUMBER
6069592

NAME AND AFFILIATION OF SUPERVISOR(S)
Dr. M.B. Rookmaaker
Division of Internal Medicine and Dermatology, Nephrology and hypertension, University Medical Center Utrecht, Utrecht

Drs. T.T. Pieters
Division of Internal Medicine and Dermatology, Nephrology and hypertension, University Medical Center Utrecht, Utrecht

Dr. A.H.M. de Vries Schultink
Division of Laboratories, Pharmacy and Biomedical Genetics, Department of Pharmacy, University Medical Center Utrecht, Utrecht

DATE OF SUBMISSION
June 30th, 2023

WORD COUNT
3543

INDEX

LIST OF ABBREVIATIONS AND RELEVANT DEFINITIONS

ALAT	alanine aminotransferase
ALL	acute lymphoblastic leukaemia
ASAT	aspartate aminotransferase
BMI	body mass index
BSA	body surface area
BW	bodyweight
CKD-EPI	Chronic Kidney Disease Epidemiology Collaboration
CL_{mtx}	methotrexate clearance
CRAFT	CT-based estimate of renal function
eGFR	estimated glomerular filtration rate
Hb	haemoglobin
HDMTX	high-dose methotrexate
Ht	haematocrit
HU	Hounsfield units
IIV	interindividual variability
LASSO	least absolute shrinkage and selection operator
MTX	methotrexate
NHL	non-Hodgkin lymphoma
NONMEM	non-linear mixed effect modelling
OFV	objective function
RA	radiation attenuation
SCR	serum creatinine concentration
UMCU	University Medical Center Utrecht
UPOD	Utrecht Patient Oriented Database
V1	volume of distribution in the central compartment
WBC	white blood count

ABSTRACT

BACKGROUND: High-dose methotrexate (HDMTX) is widely used as an established treatment for various haematological malignancies. However, prolonged exposure can lead to significant toxicity. Recent research showed the possibility to accurately estimate the creatinine clearance with the CT-based estimate of RenAl FuncTion (CRAFT) equation using automated body composition analysis of clinically obtained CT scans and automated deep learning algorithms.

Based on existing pharmacokinetic models for HDMTX, this study investigated the added value of incorporating the CRAFT, radiomics parameters and biometric and laboratory values for better predicting the pharmacokinetics of HDMTX.

METHODS: The PREDICT-MTX study is a retrospective single centre pharmacokinetics study that included patients treated with HDMTX (≥ 500 mg/m^2) with a clinical acquired CT-scan covering the L3 segment. A population pharmacokinetics model was constructed using non-linear mixed effect modelling (NONMEM) to estimate population and individual pharmacokinetic parameters. Radiomics parameters, biometric and laboratory values were evaluated as covariates.

RESULTS: The MTX concentration–time course was best described by a three-compartment model. Significant covariates that retained in the final model were serum creatinine concentration and CRAFT on methotrexate clearance (CL_{mtx}) and white blood count and 90th percentile radiation attenuation of long spine muscles on volume of distribution in the central compartment (V1).

CONCLUSION: This is the first proof-of-concept study that uses deep learning body-composition analysis of clinically acquired CT-scans to better describe the pharmacokinetics of HDMTX. We constructed a three-compartment population pharmacokinetic model that characterised the CL_{mtx} and V1 of MTX in adult patients with various malignancies treated with HDMTX.

INTRODUCTION

High-dose methotrexate (HDMTX) is widely used as an established treatment for various haematological malignancies including acute lymphoblastic leukaemia (ALL) and non-Hodgkin lymphoma (NHL). A prospective randomised phase III trial reported a significant increase in five-year disease-free survival rate in adult patients with ALL treated with HDMTX compared to those treated with intermediate-dose MTX without any increase in severe adverse events.[1] While HDMTX plays a prominent role in the treatment of haematological malignancies, HDTMX is still accompanied by substantial toxicity such as hepato- and nephrotoxicity.[2] Current population pharmacokinetic models describe the pharmacokinetics of HDMTX in attempt to better predict HDMTX-induced toxicity, however, evaluation of relevant covariates, such as body composition, is essential to further reduce toxicity while maintaining proper efficacy.[3]

MTX is a folic acid antagonist, belonging to the group of antimetabolites, that has inhibitory effect on DNA synthesis which in high doses leads to apoptosis of tumour cells while lower doses of MTX expresses anti-inflammatory and immunosuppressive effects.[4,5] MTX is actively transported intracellular, in human leukocytes amongst others, and primarily metabolised in polyglutamated MTX that subsequently leads to inhibition of dihydrofolate reductase which is responsible for the synthesis of purines and thymidine.[6,7] MTX generally distributes throughout the body and binds to albumin in plasma, while MTX also diffuses gradually into third-space fluids e.g. ascites, resulting in an extended half-life. MTX is primarily eliminated through renal excretion, of which largely is unchanged.[7]

Dosages above 500 mg/m^2 administered through prolonged intravenous infusion are referred to as HDTMX and followed by leucovorin rescue therapy, a folate analogue, to diminish the toxic effect on normal dividing cells while preserving the antitumour effect of HDTMX.[8,9] The infusion duration of HDMTX may vary between 1-4 hours and 24 hours with leucovorin rescue therapy administered at 24 and 36 hours after start of infusion, respectively.[9,10] Management of HDMTX-induced toxicity and leucovorin rescue therapy is guided through therapeutic drug monitoring until the serum MTX concentration reaches below 0.2 µmol/L.[11] Be that as it may, prolonged exposure to high concentrations of MTX can still lead to significant toxicity, mostly due to impaired renal function.[12,13] In addition, HDMTX-induced toxicity can result in a delay of further chemotherapy treatments potentially resulting in suboptimal anticancer outcomes.

Both two- and three-compartment population pharmacokinetic models have been described for HDTMX.[14–16] Renal function including GFR, estimated creatinine clearance and serum creatinine concentration (SCR) were considered an independent indicator of MTX clearance (CL_{mtx}). Other variables that may affect volume of distribution are bodyweight (BW), body surface area (BSA), height, age, alanine aminotransferase (ALAT), and dosage regimen.[16]

Serum MTX concentration and duration of exposure depend on the dose administered, the volume of distribution and the renal clearance.[7] Despite dose reduction based on conventional estimated glomerular filtration rate (eGFR) equations, serum MTX concentrations are still elevated resulting in the manifestation of MTX-induced toxicity.[17] Renal function formulas such as the Cockcroft-Gault equation may not provide accurate estimate of creatinine clearance as it assumes a standardized muscle mass.[18] Recent research showed the possibility to accurately estimate the true creatinine clearance of patients based on clinically obtained CT scans using automated deep learning algorithms.[19] The *CT-based estimate of RenAl FuncTion* (CRAFT) equation was developed based on radiomics parameters derived from cross-sectional muscle area at L3 level which is strong associated with total body muscle volume.[20] Automated body composition analysis may also lead to better estimation of the volume of distribution, since it directly quantifies muscle and fat compartments. Current renal function formulas are more sensitive to patients with atypical body composition, whereas the CRAFT directly estimates the muscle

mass and corrects for it, resulting in a more accurate estimation of creatinine clearance.[19,21] The CRAFT equation also include age, weight, and stature and was validated in healthy kidney donors as well as patients. With help of these algorithms, we expect to better describe the pharmacokinetics of HDMTX based on a more accurate estimation of creatinine clearance and volume of distribution in order to reduce the toxicity of MTX and maximise its therapeutic effect.

Regarding the toxicity, HDMTX-induced hepatotoxicity presents as acute elevations in serum transaminases concentration up to 20-fold and mainly manifest in patients treated with HDMTX which are favourably transient and return to baseline concentration within fourteen days.[12] However, there are multiple case reports of patients with MTX-induced hepatic fibrosis which later on developed hepatocellular carcinoma with HDMTX treatment as the common denominator in their early years.[22–24] HDMTX-induced nephrotoxicity was found in 1.8% of patients with osteosarcomas treated with HDMTX with a mortality rate of 4.4%.[13] MTX can precipitate in the renal tubules and form crystals which directly induce tubular injury.[25] Furthermore, MTX can cause constriction of the afferent arterioles leading to a decreased GFR resulting in a delayed excretion and decreased clearance of MTX and other drugs which may in turn lead to increased risk of other systemic toxicity.[13] Risk factors associated with HDMTX-induced nephrotoxicity are the male sex, low serum albumin concentration and multi-drug interaction.[26] HDMTX-induced nephrotoxicity can be minimized by hydration, alkalinisation of urine and as a last resort, treatment with glucarpidase, a recombinant bacterial enzyme that converts MTX to an inactive metabolite leading to faster elimination.[27,28]

Multiple studies showed a correlation between the pharmacokinetics and pharmacodynamics of HDMTX regarding toxicity.[14,29,30] A pharmacodynamics study of HDMTX in paediatric patients found a 43% increase in risk of nephrotoxicity after an observed increase serum MTX concentration of 1 µmol/L after 24 hours compared to those without an increase in serum MTX concentration. [29] Moreover, in a cohort of adult patients with ALL, non-Hodgkin lymphomas, and osteosarcomas, a significant positive correlation was found between the dose-corrected serum MTX concentration and the incidence of acute renal insufficiency.[14] Furthermore, another study demonstrated a significant positive correlation between the individual cumulative area under the curve of MTX and the mucositis score in patients with osteosarcomas.[30] Building a pharmacokinetic model with radiomics parameters derived from deep learning-based analysis of CT-scans allows for better estimation of individual pharmacokinetics of MTX for precise dosing strategies to reduce further toxicity.

Based on existing pharmacokinetic models for HDMTX, this study investigated the added value of incorporating the CRAFT, radiomics parameters derived from clinically acquired CT-scans and biometric and laboratory values for better predicting the pharmacokinetics of HDMTX. To the extent of our knowledge, this is the first proof-of-concept study where deep learning body-composition analysis of clinically acquired CT-scans was used to better understand the pharmacokinetics of HDMTX. A population pharmacokinetic model was developed using non-linear mixed effect modelling (NONMEM) based on a retrospective cohort of patients that were treated with HDMTX between 2017 and 2022 in University Medical Center Utrecht (UMCU).

METHODS

Study design, patient population, and data extraction

The PREDICT-MTX study is a retrospective single centre pharmacokinetics study conducted in the UMCU. In order to be eligible for this study, individuals had to be (1) at least 18 years or older, (2) treated with HDMTX ≥ 500 mg/m2 in the first cycle as part of standard of care treatment, and (3) have a clinical acquired CT-scan available covering the L3 segment. Participants were excluded if the time between CT-scan and administered HDMTX were >3 months apart. Pseudonymised CT-scans were retrieved from the Research Image Archive of the UMCU. Pseudonymised biometric data and laboratory values from two weeks prior HDMTX infusion were retrieved from the Utrecht Patient Oriented Database (UPOD). All patients meeting the criteria for eligibility with concentration-versus-time data were used in the analysis.

HDMTX administration and sampling

Patients received intravenous HDMTX dosages varied from 500 mg/m^2 to 5400 mg/m^2 with an infusion duration of 1-, 2-, 4- or 24 hours according to standard of care treatment protocols. The majority of samples were collected at 24, 48 and 72 hours after start of infusion. Therapeutic drug monitoring was performed until the observed serum MTX concentration was below 0.2 µmol/L. Serum MTX concentrations were quantified using the ARK™ Methotrexate Assay, a highly specific homogeneous enzyme immunoassay by the Central Diagnostic Laboratory at the UMCU in collaboration with the Division Laboratory and Pharmacy. Serum MTX concentrations after glucarpidase administration were measured at another institution with liquid chromatography-tandem mass spectrometry and was therefore not taken in the pharmacokinetic analysis as the immunoassay used in UMCU could not distinguish between serum MTX concentration and inactive metabolite.[31] Serum MTX concentrations below the limit of quantification were included and divided by two for NONMEM.[32]

CT scan segmentations and radiomics parameters

Deep learning algorithm for body-composition analysis was developed by Quantib Body Composition and described in previous literature.[19,33] Automated segmentations of muscle and fat compartments were performed at L3 level and radiomics parameters were calculated based on the Hounsfield Units (HU) distribution of these compartments. The muscles were segmented into psoas, long spine and abdominal wall muscles and further segmented using a threshold of >- 15 HU for muscles.[19,34] Fat compartments were segmented into subcutaneous and visceral fat. Segmentations were then manually checked for inaccuracies.

Pharmacokinetic modelling, covariate analysis and statistical analyses

Population pharmacokinetic modelling based on first-order conditional estimation method was performed in NONMEM v7.5.1 and assisted by Pirana v23.1.1 to estimate population and individual pharmacokinetic parameters. Two- and three-compartment PK models were evaluated with interindividual variability (IIV) in CL_{mtx} and volume of distribution in the central compartment (V1). Interoccasion variability was not determined since all patients were treated in the first cycle. The model of Ibarra et al. was used as starting point for the base model and included BW as a covariate on all parameters centred for a 70 kg individual and using an exponent of 1.0 for V1 and 0.75 for compartmental clearance and clearance parameters by means of a power model.[14]

After estimation of V1 and CL_{mtx} from the base model, Least Absolute Shrinkage and Selection Operator (LASSO) regression was used to select relevant radiomics parameters that correlated with V1. From the 208 radiomics parameters obtained from L3 on the CT-scans, 114 parameters were considered as potential predictors to be used in the LASSO regression based on expected relevance.

Remaining radiomics parameters alongside biometric data and laboratory values were evaluated as covariates on the base model. Potential biometric and laboratory covariates included sex, age, stature, BW, BMI, BSA, SCR, albumin, Cockcroft Gault, CKD-EPI 2009 and 2021, CRAFT, haemoglobin, haematocrit, white blood count (WBC), platelet count, ALAT, aspartate aminotransferase (ASAT) and total bilirubin. Renal function formulas were normalised and adjusted for BSA if necessary and the CRAFT was converted to mL/min. The covariates were evaluated using the stepwise covariate model building procedure via Perl speaks NONMEM. Based on forward selection, covariates were included if a decrease of 3.84 in the OFV ($P < 0.05$) was observed.

The final model was evaluated by change in the objective function (OFV), inspection of goodness-of-fit plots for precision and visual predictive checks for both bias and precision. Bootstrapping was done (n=1000) to calculate the 95 percent confidence interval of the final parameter estimates. Data handling and statistical analyses were carried out in R (R Foundation for Statistical Computing, Vienna, Austria) and RStudio v1.446. Mean along with standard deviation was used for normal distributed data and median with interquartile range for non-normal distributed data. P-value of <0.05 was considered statistically significant.

RESULTS

Clinical characteristics

A total of 57 patients with 140 available serum MTX concentrations were included in the analysis. One patient received glucarpidase 48 hours after HDMTX infusion. Twenty-one patients were female (36.8%) and 36 were male (63.2%) with a median age of 60.5 years (46.1-70.1). Forty-seven patients were diagnosed with non-Hodgkin lymphoma, nine patients with acute lymphoblastic leukaemia and one with chronic lymphocytic leukaemia. The baseline characteristics including biometric, general radiological and laboratory values of patients are summarised in table 1.

Table 1. Baseline characteristics including biometric, radiological and laboratory values of patients treated with high-dose methotrexate (HDMTX). Values are expressed as n(%), mean ± standard deviation or median (interquartile range).

	All participants (n = 57)
Diagnosis	
Acute lymphoblastic leukaemia	9 (15.8%)
Non-Hodgkin lymphoma	47 (82.4%)
Other	1 (1.8%)
Biometric parameters	
Female, n (%)	21 (36.8%)
Age, years	60.5 (46.1 - 70.1)
Stature, cm	176.0 (168.0 - 184.0)
Weight, kg	79.1 ± 13.3
BMI, kg/m^2	25.9 (22.8 - 28.4)
BSA, m^2	1.9 (1.8 - 2.1)
Radiomics parameters	
Psoas volume > -15 HU, cm^2	17.8 ± 6.0
Psoas mean RA > -15 HU, HU	45.9 ± 7.2
Long spine volume > -15 HU, cm^2	44.0 ± 12.1
Long spine mean RA > -15 HU, HU	40.0 ± 12.9
Abdominal wall volume > -15 HU, cm^2	64.8 ± 17.3
Abdominal wall mean RA > -15 HU, HU	33.3 ± 8.7
Laboratory values	
Creatinine, µmol/L	61.0 (52.0 - 75.0)
Cockcroft Gault, mL/min	125.7 ± 42.6
CKD-EPI (2009), mL/min[a, b]	111.0 ± 27.6
CKD-EPI (2021), mL/min[b]	113.9 ± 26.3
CRAFT, mL/min	126.6 ± 42.7
Albumin, g/L	35.6 ± 4.8
Hb, mmol/L	7.3 (6.1 - 8.5)
Ht, L/L	0.35 ± 0.07
WBC, $\cdot 10^9/L$	7.8 (3.0 - 12.8)
PC, $\cdot 10^9/L$	230.0 (151.0 - 309.0)
ALAT, U/L	29.0 (18.0 - 48.0)
ASAT, U/L	20.0 (17.0 - 26.0)
Total bilirubin, µmol/L	9.0 (7.0 - 12.0)

ALAT: alanine transaminase; ASAT: aspartate transaminase; BMI: body mass index; BSA: body surface area (Du Bois Method); CKD-EPI: Chronic Kidney Disease Epidemiology Collaboration; CRAFT: CT-based estimate of RenAl FuncTion; Hb: haemoglobin; Ht: haematocrit; HU: Hounsfield units; PC: platelet count; RA: radiation attenuation; WBC: white blood count.
[a]: Caucasian race used as default**;** [b]: normalised and adjusted for BSA.

Model building, radiomics parameter selection and covariate analysis

Following the evaluation of two- and three compartment models, the MTX concentration–time course was best described by a three-compartment model (ΔOFV = -41). Based on the three-compartment model, the V1 was estimated with IIV and used for the LASSO regression.

The LASSO for variable selection resulted in six radiomics parameters after tenfold-cross-validation which included visceral fat, abdominal wall muscles (> -15 HU), long spine muscles (> -15 HU), 90th percentile radiation attenuation (RA) of long spine muscles (> -15 HU), skewness HU of long spine muscles and skewness of the psoas muscle (> -15 HU). The corresponding coefficients are shown in Supplemental Table 1. These six radiomics parameters and CRAFT were included in the covariate analysis on V1 using the stepwise covariate model building procedure.

According to the univariate analysis, the following covariates were considered to be significantly correlated to CL_{mtx}: SCR, CRAFT, Cockcroft Gault estimated creatinine clearance, eGFR (CKD-EPI 2009 and 2021), WBC and age. The significant covariates related to V1 were SCR, CRAFT, Cockcroft Gault estimated creatinine clearance, eGFR (CKD-EPI 2009 and 2021), WBC, age, visceral fat, abdominal wall muscles (> -15 HU), 90th percentile RA of long spine muscles (> -15 HU) and long spine muscles (> -15 HU). The OFV of the significant covariates are shown in Table 2.

Table 2. Covariates correlated to the methotrexate clearance (CL_{mtx}) and volume of distribution in the central compartment (V1) in the base model. Values are expressed as difference in OFV.

Covariates	**CL_{mtx}**		**V1**	
	ΔOFV	P-value	ΔOFV	P-value
SCR	-41.00	<0.001	-18.49	<0.001
CRAFT	-25.25	<0.001	-15.37	<0.001
Cockcroft Gault	-30.64	<0.001	-17.99	<0.001
CKD-EPI 2009	-25.84	<0.001	-14.82	<0.001
CKD-EPI 2021	-24.34	<0.001	-13.60	<0.001
WBC	-6.01	<0.05	-29.71	<0.001
Age	-5.41	< 0.05	-19.10	<0.001
Visceral fat			-7.86	<0.05
Abdominal wall muscles > -15 HU			-12.13	<0.001
90^{th} percentile RA of long spine muscles > -15 HU			-14.25	<0.001
Long spine muscles > -15 HU			-13.07	<0.001

CL_{mtx}: MTX clearance; CKD-EPI: Chronic Kidney Disease Epidemiology Collaboration; CRAFT: CT-based estimate of renal function; HU: Hounsfield units; OFV: objective function; RA: radiation attenuation; SRC: serum creatinine concentration; V1: volume of distribution in the central compartment; WBC: white blood count. $p < 0.05$ is considered statistically significant and < 0.001 as statistically highly significant.

SCR on CL_{mtx} had the greatest OFV drop (ΔOFV = -41) and was therefore kept in the model. Likewise, WBC on V1 had a significant decrease in OFV (ΔOFV = -30) and was also included in the model. Based on further forward selection on the base model including SCR on CL_{mtx}, the covariates CRAFT on CL_{mtx} and 90^{th} percentile RA of long spine muscles on V1 were selected for the final model. Thus, significant covariates that retained in the final model (ΔOFV = -75) were SCR and CRAFT on CL_{mtx} and WBC and 90th percentile RA long spine muscles on V1. The final model parameter estimations are summarised in table 3 with parameter estimates well within the 95 percent confidence interval of the bootstrap estimates, which demonstrated minimal bias though with broad confidence interval ranges.

Notably, while other renal function equations were more significant correlated in the univariate analysis, during model building, the effect of CRAFT on CL_{mtx} in the final model was the greatest compared to other renal function equations after including SCR on CL_{mtx} (CRAFT with ΔOFV = -7 and CKD-EPI 2021 with ΔOFV = -4). From the four radiomics parameters that were significant in the covariate analysis, only one parameter retained in the final model. From all the laboratory values considered in the covariate analysis, only WBC was found to be significant on V1. Other covariates such as BW, BSA, height, age and ALAT did not correlate.

Table 3. Parameter estimates of the final population pharmacokinetic model of HDMTX.

Parameter	Value	95% confidence interval
CL_{pop} (L/h)	6.61	4.25 – 15.90
SCR on CL_{mtx}	-0.701	-0.949 – -0.325
CRAFT on CL_{mtx}	0.241	0.023 – 0.529
V1 (L)	15	4.04 – 46.76
90^{th} percentile RA long spine muscles > -15 HU on V1	2.07	0.572 – 6.098
WBC on V1	0.347	0.116 – 1.178
Q2 (L/h)	0.316	0.163 – 2.083
V2 (L)	2.49	1.450 – 11.861
Q3 (L/h)	0.0552	0.026 – 0.417
V3 (L)	5.78	1.20 – 64.48
IIV CL (%)	24.8	18.2 – 29.5
IIV V1 (%)	0.07	0.069 – 0.072
Residual variability	0.0661	0.0422 – 0.0859

CL_{pop}: population estimate of clearance; CL_{mtx}: methotrexate clearance; HDMTX: high-dose methotrexate; IIV: inter-individual variability; Q2 and Q3: intercompartmental clearances; RA: radiation attenuation; SRC: serum creatinine concentration; V1: volume of distribution in the central compartment; V2, and V3: volume of distribution in the peripheral compartments; WBC: white blood count.

The equation of the final model for CL and V1 was described as follows:

$$CL_i = 6.61 \cdot \left(\frac{\text{SCR}_i}{61}\right)^{-0.701} \cdot \left(\frac{\text{CRAFT}_i}{126}\right)^{0.241}$$

and

$$V1_i = 15 \cdot \left(\frac{WBC_i}{6.8}\right)^{0.347} \cdot \left(\frac{-90\text{th percentile RA long spine muscles}_i}{20}\right)^{2.07}$$

CL_i stands for the individual predicted CL_{mtx}, SCR_i represents the individual SCR in µmol/L and CRAFT_i is the computed creatinine clearance in mL/min. The $V1_i$ is the individual predicted V1, the WBC_i stands for the WBC in $\cdot 10^9$/L and the $90\text{th percentile RA long spine muscles}_i$ represents the radiomic parameter in HU. In the final model, SCR was centred on 61 µmol/L, CRAFT on 126 mL/min, WBC on 6.8 $\cdot 10^9$/L and 90th percentile RA long spines muscles on 20 HU.

The visual predictive check in figure 1 present the final three-compartment model prediction of serum MTX concentration. Majority of the observed serum MTX concentration fell between the 5th and 95th percentiles of the predicted serum MTX concentration with marginal bias. The goodness-of-fit plots of the final model with minimal bias are shown in supplemental figure 1.

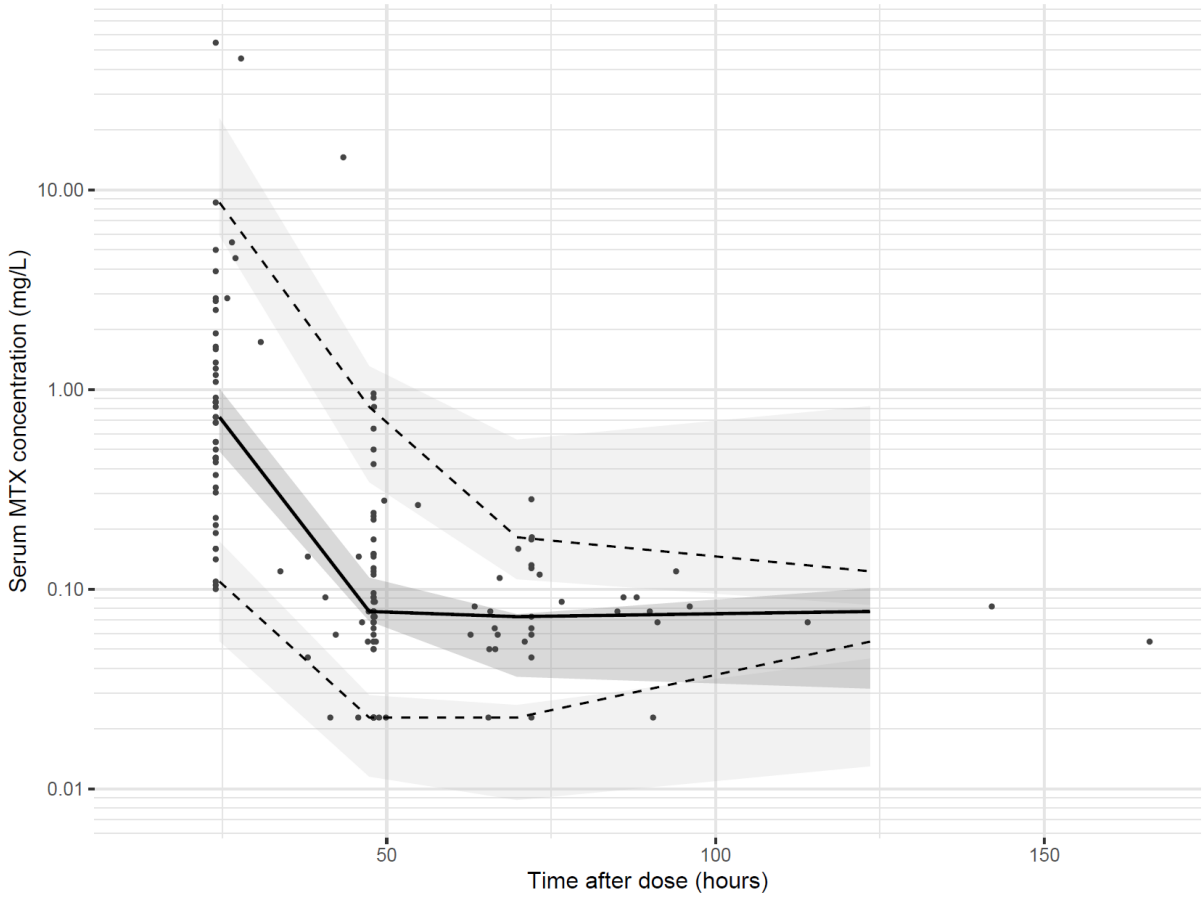

Figure 1. The visual predictive check of the final model with log-transformed serum MTX concentration in mg/L on the Y-axis and time after dose in hours on the X-axis. The observed serum MTX concentrations are shown as dots, the dashed lines present the 5th and 95th percentiles of the predicted serum MTX concentrations. The solid black line presents the median serum MTX predicted concentrations with the prediction intervals in grey.

DISCUSSION

This is the first study that uses deep learning body-composition analysis of clinically acquired CT-scans to better describe the pharmacokinetics of HDMTX. A population pharmacokinetic model for HDMTX was developed and was best characterized by a three-compartment model. SCR and CRAFT were independent predictors of CL_{mtx} while WBC and 90th percentile RA long spine muscles were independent predictors of V1. Although multiple renal function equations were significant correlated in the univariate analysis, the CRAFT in the final model was eventually the better predictor of CL_{mtx}. The use of radiomics parameters derived from clinically acquired CT-scans and CRAFT equation in this model provide a more accurate description of the pharmacokinetics of HDMTX compared to previous published pharmacokinetic models and thus may help further in the prevention of HDMTX-induced toxicity.

The effect of SCR on CL_{mtx} as independent predictor was described in both two- and three compartment models and was consistent with previous literature.[35,36] In similar fashion, the influence of renal function formulas on CL_{mtx} also corresponded with multiple pharmacokinetics reports whereupon the Cockcroft Gault equation was frequently used.[15,37] The prominent finding in this report revealed the CRAFT to be a better predictor of CL_{mtx} compared to other equations. The findings in Pieters et al. revealed the CRAFT equation to be significantly more accurate than the Cockcroft Gault equation in the estimation of creatinine clearance in healthy kidney donors.[19] The univariate analysis in this study found the Cockcroft Gault estimated creatinine clearance as potential covariate on CL_{mtx}, however, after SCR was added to the base model, it was no longer correlated with CL_{mtx}. Instead, the CRAFT was a better predictor of CL_{mtx} and was therefore included in the final model. Only 90th percentile RA long spine muscles from the six radiomics parameters was selected as independent predictor for V1. In Pieters et al., this was also the same radiomics parameter that was selected after the LASSO. The same radiomics parameter was subsequently used as a main variable in the CRAFT equation. [19]

BW, a relevant covariate, was not correlated with either CL_{mtx} or V1 which was inconsistent with previous reports.[16] BW not correlating as covariate may partially be due to the initial parameters used as starting point for the base model that were scaled by BW in Ibarra et al. An unexpected covariate with effect on V1 was WBC which has not been previously reported. Increased WBC could suggest ongoing inflammation in which inflammatory response can lead to increased vascular permeability which can be accompanied by leakage of plasma, and thus possibly MTX, into the tissues. While no relationship has ever been described between WBC and V1, there was a relationship reported between ALAT and V1 in another study.[15] Considering that MTXs bind to proteins such as albumin in plasma, increased ALAT could suggest liver dysfunction which can lead to reduced serum album concentration and therefore may affect the binding of methotrexate in both the central and peripheral compartments. However, the effect of ALAT on V1 in this study was not found. In this regard, liver enzymes measured in this report were only mildly elevated. Given that the magnitude of liver enzyme elevations indicate liver dysfunction, evident liver injury is mainly present when ALAT is significantly increased.[38] In this study, this was not the case with also serum albumin concentration being within the normal range.

The pharmacokinetics of HDMTX in this report was best described by a three-compartment model which is in accordance with earlier findings.[36,39] However, the majority of published articles on pharmacokinetic models of MTX describe a two-compartment model.[16] The elimination of MTX consist of three stages with the first half-life corresponding to the distribution phase, the second half-life being determined by the renal clearance and the third half-life determining the severity of toxicity.[40,41] A three compartment model is able to more accurately describe the pharmacokinetics of a drug demonstrating three phases of elimination.

A limitation of this study was the relatively small sample size used in the analysis. Estimating the variability of pharmacokinetic parameters and extrapolating these findings to a broader population can

be challenging and should be done with caution. Regardless, numerous pharmacokinetics studies have used small cohorts.[42–44] Furthermore, time between HDMTX administration and CT scan was up till three months for inclusion. Changes may have happened to the body-composition of patients during that time period, in particular when diagnosed with (haematological) malignancies and treated with chemotherapy. This may lead to less accurate radiomics data when compared to the moment of HDMTX administration. However, radiomics parameters of clinically acquired CT scan give a more detailed representation of a patient's body composition compared to standard biometric data. Lastly, external model validation was not assessed during this study and is required before implementation in any standard of care treatment.

In future research, an external model validation should be performed to evaluate this model and to assess the predictive accuracy of this pharmacokinetic model for future application in clinical practice. Finally, the CRAFT and the radiomics parameter from clinically acquired CT scans has proven to be valued additions to the pharmacokinetic model as it helps to better describe the pharmacokinetics of HDMTX. Therefore, it is appropriate to further investigate the added value of the CRAFT and radiomics parameters in various pharmacokinetic models of drugs with increased toxicity that depend on the volume of distribution or renal clearance. Following this, the relationship between the exposure and toxicity of HDMTX can be further investigated with the incorporated CRAFT and radiomics to build a pharmacokinetic-pharmacodynamic model using NONMEM.

In conclusion, we constructed a three-compartment population pharmacokinetic model that characterised the CL_{mtx} and V1 of MTX in adult patients with various malignancies treated with HDMTX. The SCR, CRAFT, WBC and 90^{th} percentile RA long spine muscles were seen as relevant covariates in the final model. The next step is to externally validate this model and prospectively implement it in future routine clinical care and to further benefit from clinically acquired CT scans to describe the pharmacokinetics of other various drugs.

REFERENCES

1. Sakura T, Hayakawa F, Sugiura I, Murayama T, Imai K, Usui N, et al. High-dose methotrexate therapy significantly improved survival of adult acute lymphoblastic leukemia: A phase III study by JALSG. Leukemia. 2018 Mar 1;32(3):626–32.

2. Gökbuget N, Hoelzer D. High-dose methotrexate in the treatment of adult acute lymphoblastic leukemia. Ann Hematol. 1996 Apr 19;72(4):194–201.

3. Orgel E, Nabais T, Douglas C, Mittelman SD, Neely M. Effect of Body Fat on Population Pharmacokinetics of High-Dose Methotrexate in Pediatric Patients With Acute Lymphoblastic Leukemia. J Clin Pharmacol. 2021 Jun 1;61(6):755–62.

4. Cronstein BN, Aune TM. Methotrexate and its mechanisms of action in inflammatory arthritis. Vol. 16, Nature Reviews Rheumatology. Nature Research; 2020. p. 145–54.

5. Genestier L, Paillot R, Quemeneur L, Izeradjene K, Revillard JP. Mechanisms of action of methotrexate [Internet]. Vol. 47, Immunopharmacology. 2000. Available from: www.elsevier.comrlocaterimmpharm

6. Quéméneur L, Gerland LM, Flacher M, Ffrench M, Revillard JP, Genestier L. Differential Control of Cell Cycle, Proliferation, and Survival of Primary T Lymphocytes by Purine and Pyrimidine Nucleotides. The Journal of Immunology. 2003 May 15;170(10):4986–95.

7. Bleyer WA. Methotrexate: clinical pharmacology, current status and therapeutic guidelinest. Vol. 4, Cancer Treatment Reviews. 1977.

8. Goldin A, Venditti JM, Kline I, Mantel N. Eradication Of Leukaemic Cells (L1210) by Methotrexate and Methotrexate Plus Citrovorum Factor. Nature. 1966 Dec 1;212(5070):1548–50.

9. Howard SC, McCormick J, Pui CH, Buddington RK, Harvey RD. Preventing and Managing Toxicities of High-Dose Methotrexate. Oncologist. 2016 Dec 1;21(12):1471–82.

10. Cohen IJ, Wolff JE. How long can folinic acid rescue be delayed after high-dose methotrexate without toxicity? Vol. 61, Pediatric Blood and Cancer. John Wiley and Sons Inc.; 2014. p. 7–10.

11. Song Z, Hu Y, Liu S, Wang G, Zhai S, Zhang X, et al. Medication therapy of high-dose methotrexate: An evidence-based practice guideline of the Division of Therapeutic Drug Monitoring, Chinese Pharmacological Society. Br J Clin Pharmacol. 2022 May 1;88(5):2456–72.

12. Green MR, Chowdhary S, Lombardi KM, Chalmers LM, Chamberlain M. Clinical utility and pharmacology of high-dose methotrexate in the treatment of primary CNS lymphoma. Vol. 6, Expert Review of Neurotherapeutics. 2006. p. 635–52.

13. Widemann BC, Balis FM, Kempf-Bielack B, Bielack S, Pratt CB, Ferrari S, et al. High-Dose Methotrexate-Induced Nephrotoxicity in Patients with Osteosarcoma: Incidence, Treatment, and Outcome. Vol. 100, Cancer. 2004. p. 2222–32.

14. Ibarra M, Combs R, Taylor ZL, Ramsey LB, Mikkelsen T, Buddington RK, et al. Insights from a pharmacometric analysis of HDMTX in adults with cancer: Clinically relevant covariates for application in precision dosing. Br J Clin Pharmacol. 2023 Feb 1;89(2):660–71.

15. Kawakatsu S, Nikanjam M, Lin M, Le S, Saunders I, Kuo DJ, et al. Population pharmacokinetic analysis of high-dose methotrexate in pediatric and adult oncology patients. Cancer Chemother Pharmacol. 2019 Dec 1;84(6):1339–48.

16. Zhang Y, Sun L, Chen X, Zhao L, Wang X, Zhao Z, et al. A Systematic Review of Population Pharmacokinetic Models of Methotrexate. Eur J Drug Metab Pharmacokinet. 2022 Mar 5;47(2):143–64.

17. Herrlinger U, Schabet M, Brugger W, Kortmann RD, Küker W, Deckert M, et al. German Cancer Society Neuro-Oncology Working Group NOA-03 multicenter trial of single-agent high-dose methotrexate for primary central nervous system lymphoma. Ann Neurol. 2002;51(2):247–52.

18. Cockcroft DW, Henry M, Ault G. Prediction of Creatinine Clearance from Serum Creatinine1. Vol. 1, Nephron. 1976.

19. Pieters TT, Veldhuis WB, Moeskops P, de Vos BD, Verhaar MC, Haitjema S, et al. Deep learning body-composition analysis of clinically acquired CT-scans estimates creatinine excretion with high accuracy in patients and healthy individuals. Sci Rep. 2022 Dec 1;12(1).

20. Moeskops P, de Vos B, Veldhuis. W.B., de Jong PA, Išgum I, Leiner T. Automatic quantification of body composition at L3 vertebra level with convolutional neural networks. European Congress of Radiology. 2020;

21. Eppenga WL, Kramers C, Derijks HJ, Wensing M, Wetzels JFM, De Smet PAGM. Individualizing pharmacotherapy in patients with renal impairment: The validity of the modification of diet in renal disease formula in specific patient populations with a glomerular filtration rate below 60 ml/min. A systematic review. PLoS One. 2015 Mar 5;10(3).

22. Fried M, Kalra J, Ilardi CF, Sawitsky A. Hepatocellular carcinoma in a long-term survivor of acute lymphocytic leukemia. Cancer. 1987 Nov 15;60(10):2548–52.

23. Ruymann BF, Mosijczuk MAD, Sayers RJ. Hepatoma in a child with methotrexate-induced hepatic fibrosis. J Am Med Assoc. 1977 Dec 12;238(24):2631–3.

24. Kumari TP, Shanvas A, Mathews A, Kusumakumary P. Hepatocellular Carcinoma: A Rare Late Event in Childhood Acute Lymphoblastic Leukemia. J Pediatr Hematol Oncol [Internet]. 2000;22(3). Available from: https://journals.lww.com/jpho-online/Fulltext/2000/05000/Hepatocellular_Carcinoma__A_Rare_Late_Event_in.21.aspx

25. Garneau AP, Riopel J, Isenring P. Acute Methotrexate-Induced Crystal Nephropathy. New England Journal of Medicine. 2015 Dec 31;373(27):2691–3.

26. Wiczer T, Dotson E, Tuten A, Phillips G, Maddocks K. Evaluation of incidence and risk factors for high-dose methotrexate-induced nephrotoxicity. Journal of Oncology Pharmacy Practice. 2016 Jun 1;22(3):430–6.

27. Feinsilber D, Leoni RJ, Siripala D, Leuck J, Mears KA. Evaluation, Identification, and Management of Acute Methotrexate Toxicity in High-dose Methotrexate Administration in Hematologic Malignancies. Cureus. 2018 Jan 8;

28. Fermiano M, Bergsbaken J, Kolesar JM. Glucarpidase for the management of elevated methotrexate levels in patients with impaired renal function. Vol. 71, American Journal of Health-System Pharmacy. American Society of Health-Systems Pharmacy; 2014. p. 793–8.

29. Aquerreta I, Aldaz A, Giráldez J, Sierrasesúmaga L. Pharmacodynamics of High-Dose Methotrexate in Pediatric Patients. Annals of Pharmacotherapy. 2002 Sep 28;36(9):1344–50.

30. Johansson ÅM, Hill N, Perisoglou M, Whelan J, Karlsson MO, Standing JF. A Population Pharmacokinetic/Pharmacodynamic Model of Methotrexate and Mucositis Scores in Osteosarcoma. Ther Drug Monit. 2011 Dec;33(6):711–8.

31. Al-Turkmani MR, Law T, Narla A, Kellogg MD. Difficulty measuring methotrexate in a patient with high-dose methotrexate-induced nephrotoxicity. Clin Chem. 2010 Dec;56(12):1792–4.

32. Bergstrand M, Karlsson MO. Handling data below the limit of quantification in mixed effect models. AAPS Journal. 2009;11(2):371–80.

33. Mourtzakis M, Prado CMM, Lieffers JR, Reiman T, McCargar LJ, Baracos VE. A practical and precise approach to quantification of body composition in cancer patients using computed tomography images acquired during routine care. Applied Physiology, Nutrition and Metabolism. 2008 Oct;33(5):997–1006.

34. Engelke K, Museyko O, Wang L, Laredo JD. Quantitative analysis of skeletal muscle by computed tomography imaging—State of the art. Vol. 15, Journal of Orthopaedic Translation. Elsevier (Singapore) Pte Ltd; 2018. p. 91–103.

35. Mei S, Li X, Jiang X, Yu K, Lin S, Zhao Z. Population Pharmacokinetics of High-Dose Methotrexate in Patients With Primary Central Nervous System Lymphoma. J Pharm Sci. 2018 May 1;107(5):1454–60.

36. Taylor ZL, Mizuno T, Punt NC, Baskaran B, Navarro Sainz A, Shuman W, et al. MTXPK.org: A Clinical Decision Support Tool Evaluating High-Dose Methotrexate Pharmacokinetics to Inform Post-Infusion Care and Use of Glucarpidase. Clin Pharmacol Ther. 2020 Sep 1;108(3):635–43.

37. Kim IW, Yun H yeol, Choi B, Han N, Park SY, Lee ES, et al. ABCB1 C3435T Genetic Polymorphism on Population Pharmacokinetics of Methotrexate After Hematopoietic Stem Cell Transplantation in Korean Patients: A Prospective Analysis. Clin Ther. 2012 Aug;34(8):1816–26.

38. Giannini EG, Testa R, Savarino V. Liver enzyme alteration: A guide for clinicians. Vol. 172, CMAJ. Canadian Medical Association Journal. Canadian Medical Association; 2005. p. 367–79.

39. Simon N, Marsot A, Villard E, Choquet S, Khe HX, Zahr N, et al. Impact of ABCC2 polymorphisms on high-dose methotrexate pharmacokinetics in patients with lymphoid malignancy. Pharmacogenomics Journal. 2013 Dec;13(6):507–13.

40. Wilhem AJ. TDM Monografie informatie Methotrexaat (MTX) [Internet]. Commissie Analyse & Toxicologie van de Nederlandse Vereniging van Ziekenhuisapothekers. 2011. Available from: https://tdm-monografie.org/methotrexaat-mtx/

41. Blum R, Seymour JF, Toner G. Significant impairment of high-dose methotrexate clearance following vancomycin administration in the absence of overt renal impairment. Annals of Oncology. 2002;13(2):327–30.

42. Nader A, Zahran N, Alshammaa A, Altaweel H, Kassem N, Wilby KJ. Population Pharmacokinetics of Intravenous Methotrexate in Patients with Hematological Malignancies: Utilization of Routine Clinical Monitoring Parameters. Eur J Drug Metab Pharmacokinet. 2017 Apr 1;42(2):221–8.

43. Fukuhara K, Ikawa K, Morikawa N, Kumagai K. Population pharmacokinetics of high-dose methotrexate in Japanese adult patients with malignancies: a concurrent analysis of the serum and urine concentration data. J Clin Pharm Ther. 2008 Dec;33(6):677–84.

44. Hui KH, Chu HM, Fong PS, Cheng WTF, Lam TN. Population Pharmacokinetic Study and Individual Dose Adjustments of High-Dose Methotrexate in Chinese Pediatric Patients With Acute Lymphoblastic Leukemia or Osteosarcoma. J Clin Pharmacol. 2019 Apr 1;59(4):566–77.

SUPPLEMENTARY METERIAL

Supplemental Table 1. Coefficient of the radiomics parameters that were remained using LASSO.

Parameters	Coefficient
Intercept	10.43384
Visceral fat, cm^2	0.00005914734
Skewness > -15 HU Psoas muscles, HU	0.1787959
Abdominal wall muscles > -15 HU, cm^2	0.01118747
Skewness HU Long spine muscles, HU	0.09584292
90^{th} percentile RA long spine muscles > -15 HU, HU	-0.2141822
Long spine muscles > -15 HU, cm^2	0.001742469

HU: Hounsfield Unit; RA: radiation attenuation

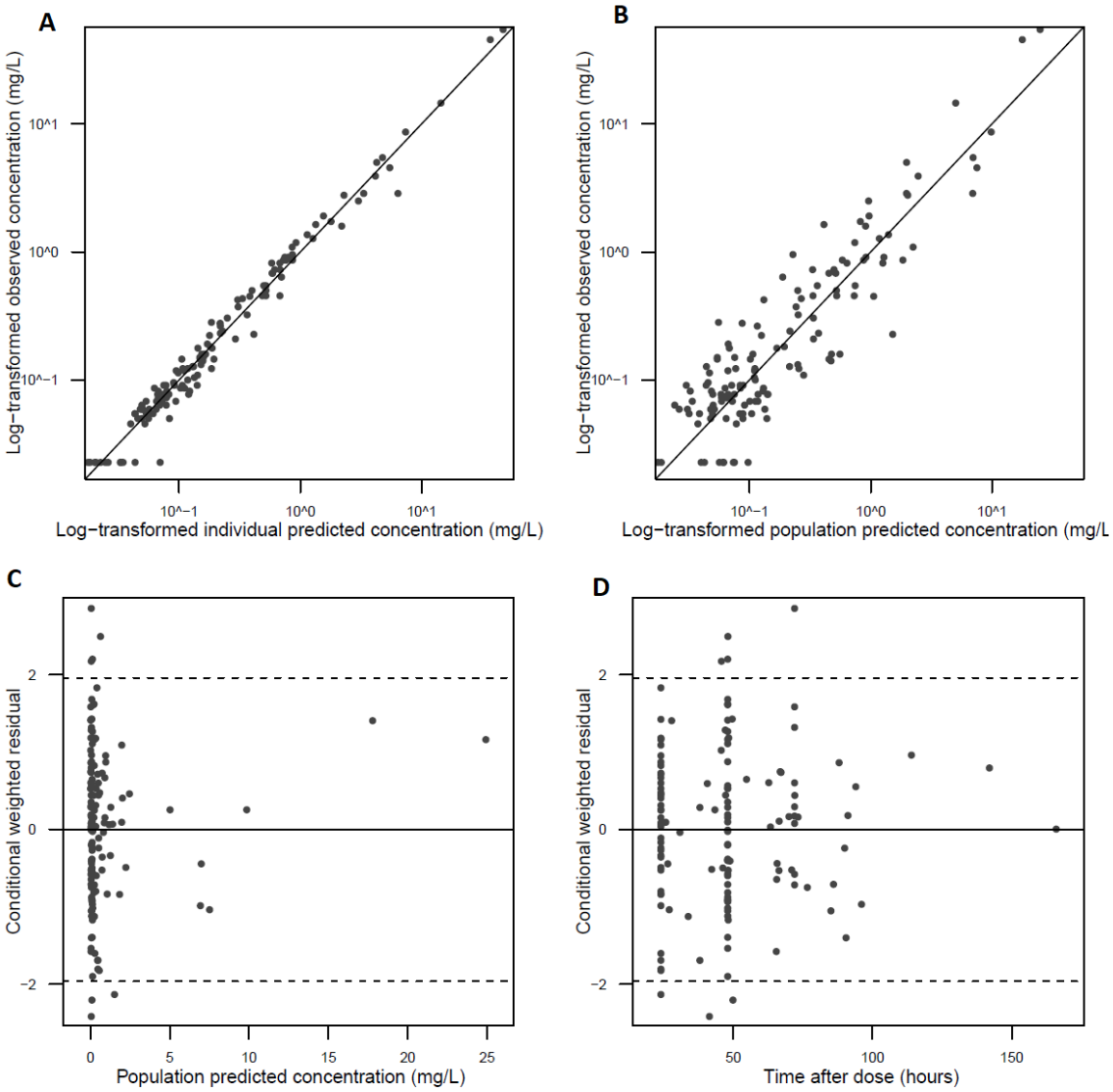

Supplemental figure 1. The goodness-of-fit plots of the final model. Shown are (A) the observed vs predicted serum MTX concentration of individuals, (B) the observed vs the population predicted serum MTX concentration, (C) the distribution of conditional weighted residuals vs population predicted serum MTX concentration and (D) the distribution of conditional weighted residuals vs time after dose in hours. The observed and predicted serum MTX concentrations are shown in mg/L.